

Reply to comments of Topic Editor

The topic editor knows the topic very well and his comments are indeed helpful in improving the quality of this MS. We are grateful to Prof. John M. Huthnance for a careful checking and comments on the MS. All comments are addressed point by point, each starting with an original comment and followed by a response in italic, as follows.

Topic Editor Decision: Publish subject to minor revisions (review by editor) (20 Feb 2019) by John M. Huthnance

Comments to the Author:

Dear Authors.

Thank-you for your revised manuscript. I still have trouble with some of your statements about (non) stationarity and especially nonlinearity as detailed in “Comments” below. Referee 1 (Huang) also commented on this and I think you have not yet addressed all his comments. He also asked for a comparison with the results of EMD-BPNN (his point 1) and demonstration that there is a mode mixing problem with EMD (his point 2); you respond to these points in your response but in the revised paper I do not see either of what is asked for. Also at the end of your response to referee 2 you say “We have stated some factors affecting the SST prediction in the revised manuscript” but I do not see any more about this in the revised manuscript. Hence I am still asking for “minor” revision and wish to see the manuscript again myself. Please also note that all comments will be available when any final version is published and readers will be able to see how you have addressed them.

Yours sincerely

John Huthnance

***Response:** Thank you for these comments. On behalf of my co-authors, we thank Prof. John M. Huthnance very much for giving us an opportunity to revise our manuscript, we appreciate editor and reviewers very much for their positive and constructive comments and suggestions on our manuscript.*

We elaborated and compared the results of different SST predictions based on the two improved EMD methods in Sections 3.1 and 3.2 and Section 5 Case study. We knew that once an intermittent signal appears in the actual signal, the EMD decomposition method would produce a Mode Mixing Problem based on previous literature such as Colominas et al. (2012), Wang et al. (2012) and Tang et al. (2015). The Mode Mixing Problem causes the essential modal function to lose its physical meaning.

Factors affecting the SST prediction results include: the length and interval of the time series of the database, as well as different sample sources because their values are also different. We added the relevant explanations in the conclusions.

References:

Colominas M A, Schlotthauer G, TORRES M E, et al. Noise-assisted EMD methods in action[J]. Advances in Adaptive Data Analysis, 2012, 4(04): 1250025.

Wang T, Zhang M, Yu Q, et al. Comparing the applications of EMD and EEMD on time–frequency analysis of seismic signal[J]. Journal of Applied Geophysics, 2012, 83: 29-34.

Tang L, Dai W, Yu L, et al. A novel CEEMD-based EELM ensemble learning paradigm for crude oil price forecasting[J]. International Journal of Information Technology & Decision Making, 2015, 14(01): 141-169.

Comments

Line 9. Please delete “novel” (Referee 1)

Response: Thank you for the suggestion. We removed it.

Lines 48-49. “. . the nonlinear and non-stationary characteristics are obvious.” You have not yet defined “non-linear”! The definition is in lines 51-52: “the change of the output is not proportional to the change of the input”. To claim “nonlinear” you need evidence that the SST is not proportional to its “input” – what is the input? I agree the SST is “non-stationary” but not because of “high randomness” so not “due to” (line 47).

Response: Thank you for the comment. Since SST changes are high randomness and irregular, we consider SST to be non-linear and non-stationary.

Line 56. “deterministic” here but “high randomness” in line 48. Which?

Response: Thank you for the comment. “deterministic” here means the “clearly” high randomness.

Line 56. “non-linear” needs evidence.

Line 56. “non-stationary” – I agree but you have not justified this.

Response: Thank you for the comment. Since SST changes are high randomness and irregular, we consider SST to be non-linear and non-stationary. And we also can find it in many previous literatures.

Line 59. You imply that the trend is orthogonal; Referee 1 objected. Maybe “. . obtain several periodic signals orthogonal to each other and a trend.”

Line 59. Are the EMD IMFs in fact orthogonal? Lines 87-88 “decomposing it via EMD . . . In contrast to the EEMD method, the CEEMD also ensures that the IMF set is quasi-complete and orthogonal. . .” suggests EMD IMFs are not orthogonal.

Response: Thank you for the comment. The IMFs are orthogonal components, but the trending component is not orthogonal to any IMF component. We corrected it.

Lines 59-60. You can delete “the method can decompose the stronger nonlinear and non-stationary signals”; it is repeated in line 62.

Response: Thank you for the suggestion. We deleted it.

Line 67. What is “essential modal function”? Please define it. If you mean “IMF”, say “IMF”.

Response: Thank you for the comment. “essential modal function” means “IMFs” and we corrected it.

Lines 72-73. These need to make clear the difference between EEMD and CEEMD. What is the difference between the EEMD “white noise” and the CEEMD “set of noise signals”?

Response: Thank you for the comment. The difference between EMD, EEMD and CEEMD is as follows:

Empirical Mode Decomposition (EMD) is a relatively slow decomposition method and it has a problem called mode mixing. This is defined as either a single IMF consisting of widely disparate scales, or a signal of similar scale captured in different IMF's. To overcome mode mixing two noise assisted methods have emerged.

Ensemble Empirical Mode Decomposition (EEMD) adds a fixed percentage of white noise to the signal before decomposing it. This step is repeated N times after which all results are averaged. EEMD

improves the mode-mixing problem but it cannot completely reconstruct the input signal from the resulting components.

Complete Ensemble Mode Decomposition (CEEMD) is also a noise-assisted method. Similarly the method decomposes the signal with N different noise realizations but here the results are averaged after each component is found. CEEMD solves the mode mixing problem and it provides an exact reconstruction of the input signal.

(1) EMD – slow and possibly suffers from mode-mixing;

(2) EEMD – slower but partly solves mode-mixing, however signal cannot be reconstructed exactly.

(3) CEEMD – slowest but solves the mode-mixing problem and the signal can be reconstructed exactly from the components.

Lines 83-84. “can effectively reduce the non-stationarity of the time-series data”. Surely the non-stationarity has to remain somewhere in the IMFs and RES?

Response: *Thank you for the comment. Each IMF component decomposed by the every EMD method contains local characteristic signals with different time scales of the original signal.*

Lines 57-90 overall need to be properly organised as a logical sequence, EMD then EEMD then CEEMD, to avoid repetition (e.g. lines 72-73 and 74-76 describe the same thing, EEMD), clarify the differences and exactly what is orthogonal.

Response: *Thank you for the comment. The difference between EMD, EEMD and CEEMD is as follows:*

(1) Empirical Mode Decomposition (EMD) is a relatively slow decomposition method and it has a problem called mode mixing. This is defined as either a single IMF consisting of widely disparate scales, or a signal of similar scale captured in different IMF's. To overcome mode mixing two noise assisted methods have emerged. EMD – slow and possibly suffers from mode-mixing. (2) Ensemble Empirical Mode Decomposition (EEMD) adds a fixed percentage of white noise to the signal before decomposing it. This step is repeated N times after which all results are averaged. EEMD improves the mode-mixing problem but it cannot completely reconstruct the input signal from the resulting components. EEMD – slower but partly solves mode-mixing, however signal cannot be reconstructed exactly. (3) Complete Ensemble Mode Decomposition (CEEMD) is also a noise-assisted method. Similarly the method decomposes the signal with N different noise realizations but here the results are averaged after each component is found. CEEMD solves the mode mixing problem and it provides an exact reconstruction of the input signal. CEEMD – slowest but solves the mode-mixing problem and the signal can be reconstructed exactly from the components.

Lines 130-131. “. . then each IMF_{*i*} is reconstructed to obtain the predicted value of SSTA.” I think you mean “. . then the IMF_{*i*} are recombined to obtain the predicted value of SSTA.” You already have each IMF_{*i*} (line 130) so each IMF_{*i*} does not need to be “reconstructed”.

Response: *Thank you for the comment. We corrected it.*

Line 141. “still exhibit strong nonlinearity and non-stationarity”. Some non-stationarity can be seen in figure 3, e.g. sub-periods with larger and longer-period variance, but it would help if you said what non-stationarity the reader is supposed to see. Figure 3 cannot show nonlinear dependence on the input since we do not know the input.

Line 142. “the non-stationary and nonlinear properties are less”. Again, how do we see non-stationary

properties? The figure cannot show nonlinear properties since we do not know the input.

Response: Thank you for the comment. We can see that the first three intrinsic mode function components still have strong irregular oscillations and periodic changes, and so can be found out non-stationary. We removed the relevant description about the nonlinear property.

Line 144. “. . . As the non-stationarity of each IMF_i is gradually reduced, . . .” I think you mean “. . . As the non-stationarity of IMF_i decreases with increasing i, . . .”

Response: Thank you for the suggestion We corrected it.

Lines 156-157. “. . . and the order of magnitude is 10^{-3} .” This can be deleted (unnecessary) and is not an accurate description of 0.0035°C .

Response: Thank you for the suggestion We removed it.

Line 166. Delete “nonlinearities and” unless you can show non-linear dependence on an input.

Response: Thank you for the suggestion We deleted it.

Line 166. “eight” -> “seven”; the eighth series is RES which is definitely non-stationary!

Response: Thank you for the suggestion We corrected it.

Line 177. “. . . and the order of magnitude is 10^{-17} .” This can be deleted (unnecessary) and is not an accurate description of $6.10 \times 10^{-17}^{\circ}\text{C}$.

Response: Thank you for the suggestion We deleted it.

Lines 223, 225. Delete “nonlinearity” unless you can show non-linear dependence on an input.

Response: Thank you for the suggestion We deleted it.

Lines 225, 226. “since” (line 225) implies that these two lines are related. How?

Response: Thank you for the suggestion We corrected it.

Line 226. Do the “12 nodes” correspond to 12 months in the year?

Line 234. $N = 12$? Please be explicit.

Response: Thank you for the suggestion We added a supplementary explanation.

Lines 240-241. To have “error (Max ERR) of the first decomposition component IMF1” you have to have “true” 2017 values for IMF1 as well as the predicted values. You need to say how you obtain the “true” values of IMF1. It seems to imply that you did the decomposition for 1982-2017 as well as for 1982-2016. Likewise for the other IMF_i and RES. I guess the IMFs for these two decomposition periods differ in 1982-2016, although perhaps very little for IMF1 until the very end of 2016.

Response: Thank you for the comment. We have actual values for 2017, so we can use it to compare against predicted values based on actual values for 1982-2016.

Tables 1 and 2. The format of the values in any row should be the same for max/min/mean ERR and for RMSE.

Response: Thank you for the comment. But We are sorry that we did not understand this and we thought we kept the same format -- all values reserved to the last four digits of the decimal point.

Table 1 row RES. RMSE has to be greater than mean ERR. Also Mean ERR is too small; $(\text{Min ERR} \times 11 + \text{Max ERR}) / 12$ exceeds Mean ERR.

Response: Thank you for the comment. This is our typo error and we corrected it.

Line 248. Delete “nonlinearity and” unless you can show non-linear dependence on an input.

Response: Thank you for the suggestion We deleted it.

Lines 273, 274. Please state a criterion for “satisfactory” and do not change it for CCEMD. At present you imply 0.3°C for EEMD and 0.1°C for CCEMD. And include the “°C”.

Response: Thank you for the comment. Indeed, how to evaluate satisfaction is a very difficult thing. However, we believe that the error of the prediction results obtained is less than 0.1°C, which is already a very good prediction result.

Lines 281-283. Better “The correlation coefficient between the prediction values based on the CEEMD-BPNN model and observations is 0.97 indicating a significance level of 0.001. The result . . 2017 was predicted”

Response: Thank you for the comment. We corrected it.

Lines 286-287. Better “. . Table 3 shows that prediction results of the hybrid CEEMD and BPNN model are much better than with the EEMD-BPNN . .”

Response: Thank you for the comment. We corrected it.

Line 288. Delete “and nonlinear” unless you can show non-linear dependence on an input.

Response: Thank you for the comment. We corrected it.

Line 303. You can omit “respectively” (unnecessary).

Response: Thank you for the comment. We corrected it.

Line 307. “. . components (IMF1, . .”

Response: Thank you for the comment. We corrected it.

Line 308. Justify or omit “strong nonlinearity and non-stationarity. As the nonlinearity gradually decreases”

Response: Thank you for the comment. We deleted it.

Line 310. Better “. . preliminary, based . .”

Response: Thank you for the comment. We corrected it.

Hybrid improved EMD-BPNN model for the prediction of sea surface temperature

Zhiyuan Wu^{a,b,c}, Changbo Jiang^{a,c,*}, Mack Conde^d, Bin Deng^{a,c}, Jie Chen^{a,c}

a. School of Hydraulic Engineering, Changsha University of Science & Technology, Changsha, 410004, China;

b. School for Marine Science and Technology, University of Massachusetts Dartmouth, New Bedford, MA 02744, USA;

c. Key Laboratory of Water-Sediment Sciences and Water Disaster Prevention of Hunan Province, Changsha, 410004, China;

d. Department of Mathematics, University of Massachusetts Dartmouth, North Dartmouth, MA 02747, USA.

Highlights

- A ~~novel~~ SST predicting method based on the hybrid EMD algorithms and BP neural network method ~~isare~~ proposed in this paper.
- SST prediction results based on the hybrid EEMD-BPNN and CEEMD-BPNN models are compared and discussed.
- Cases study of SST in the North Pacific shows that the proposed hybrid CEEMD-BPNN model can effectively predict the time-series SST.

Abstract: Sea surface temperature (SST) is the major factor that affects the ocean-atmosphere interaction, and in turn the accurate prediction of SST is the key to ocean dynamic prediction. In this paper, an SST predicting method based on empirical mode decomposition (EMD) algorithms and back-propagation neural network (BPNN) is proposed. Two different EMD algorithms have been applied extensively for analyzing time-series SST data and some nonlinear stochastic signals. Ensemble empirical mode decomposition (EEMD) algorithm and Complementary Ensemble Empirical Mode Decomposition (CEEMD) algorithm are two improved algorithms of EMD, which can effectively handle the mode-mixing problem and decompose the original data into more stationary signals with different frequencies. Each Intrinsic Mode Function (IMF) has been taken as an input data to the back-propagation neural network model. The final predicted SST data is obtained by aggregating the predicted data of individual IMF. A case study, of the monthly mean ~~sea surface temperature~~ SST anomaly (SSTA) in the northeastern region of the North Pacific, shows that the proposed hybrid CEEMD-BPNN model is much more accurate than the hybrid EEMD-BPNN model, and the prediction accuracy based on BP neural network is improved by the CEEMD method. Statistical analysis of the case study demonstrates that applying the proposed hybrid CEEMD-BPNN model is effective for the SST

30 prediction.

31

32 **Keywords.**

33 Sea Surface Temperature; Back-Propagation Neural Network; Empirical Mode Decomposition; Prediction;
34 Machine Learning Algorithms.

35

36 **1 Introduction**

37 The Sea Surface Temperature (SST) is a main factor in the interaction between the ocean and the
38 atmosphere (Wiedermann et al., 2017; He et al., 2017; Wu et al., 2019a), and it characterizes the combined
39 results of ocean heat (Buckley et al., 2014; Griffies et al., 2015; Wu et al., 2019b), dynamic processes
40 (Takakura et al., 2018). It is a very important parameter for climate change and ocean dynamics process,
41 reflects sea-air heat and water vapor exchange. Small changes in sea temperature can have a huge impact on
42 the global climate. The well-known El Niño and La Niña phenomena are caused by abnormal changes in SST
43 (Chen et al., 2016a; Zheng et al., 2016).

44 Therefore, scholars have begun to observe the SST in recent years, the observation of the SST is
45 important (Kumar et al., 2017; Sukresno et al., 2018). Accurate observation and effective prediction of the
46 SST are very important (Hudson et al., 2010). Predicting the SST in advance can enable people to take
47 appropriate measures to reduce the impact on daily life and reduce unnecessary losses. However, due to the
48 high randomness and irregular of the monthly mean sea surface temperature anomaly (SSTA), the nonlinear
49 and non-stationary characteristics are obvious. At present, there is no clear and feasible method with high
50 accuracy to effectively predict the SST (Zhu et al., 2015; Chen et al., 2016b; Khan et al., 2017).

51 In mathematics and science, a nonlinear system is a system in which the change of the output is not
52 proportional to the change of the input. Nonlinear dynamical systems, describing changes in variables over
53 time, may appear chaotic, unpredictable, or counterintuitive, contrasting with much simpler linear systems.
54 A stationary process is a stochastic process whose unconditional joint probability distribution does not change
55 when shifted in time. Consequently, statistical parameters such as mean and variance also do not change over
56 time. The variation of SST is a deterministic non-linear dynamic system and a non-stationary time series data.
57 Empirical Mode Decomposition (EMD) is a state-of-the-art signal processing method proposed by Huang et
58 al. (1998). This method can decompose the signal data of different frequencies step by step according to the
59 characteristics of the data and obtain several orthogonal components and a trending component~~periodic and~~

60 ~~trending signals orthogonal to each other, the method can decompose the stronger nonlinear and non-~~
61 ~~stationary signals~~ (Wang et al., 2015; Amezquita-Sanchez and Adeli,2015; Wang et al., 2016; Kim and Cho,
62 2016). The empirical mode decomposition (EMD) method is powerful and adaptive in analyzing nonlinear
63 and non-stationary data sets. It provides an effective approach for decomposing a signal into a collection of
64 so-called intrinsic mode functions (IMFs), which can be treated as empirical basis functions (Duan et al.,
65 2016). However, there were some problems ~~with~~ the EMD method, such as mode mixing (Huang and Wu,
66 2008; Wu et al., 2008; Wu and Huang, 2009).

67 Once an intermittent signal appears in the actual signal, the EMD decomposition method will produce
68 a Mode Mixing Problem. The Mode Mixing Problem causes the essential modal function (IMFs) to lose its
69 physical meaning. This is defined as either a single IMF consisting of widely disparate scales, or a signal of
70 similar scale captured in different IMF's. To overcome mode mixing two noise assisted methods have
71 emerged. Ensemble Empirical Mode Decomposition (EEMD) adds a fixed percentage of white noise to the
72 signal before decomposing it. This step is repeated N times after which all results are averaged. EEMD
73 improves the mode-mixing problem but it cannot completely reconstruct the input signal from the resulting
74 components. Complete Ensemble Mode Decomposition (CEEMD) is also a noise-assisted method. Similarly
75 the method decomposes the signal with N different noise realizations but here the results are averaged after
76 each component is found. CEEMD solves the mode mixing problem and it provides an exact reconstruction
77 of the input signal.

78 ~~In addition, the Mode Mixing Problem will also make the algorithm of Empirical Mode Decomposition~~
79 ~~unstable, and any disturbance may generate a new intrinsic mode function. In order to solve this problem,~~
80 ~~scholars have proposed the use of noise assisted processing methods, Ensemble empirical mode~~
81 ~~decomposition (EEMD) and Complementary Ensemble Empirical Mode Decomposition (CEEMD). The~~
82 ~~white noise has been added to the original signal to change the extreme point distribution of the signal in the~~
83 ~~EEMD method, while in the CEEMD method, a set of noise signals have been added to the original signal to~~
84 ~~change the extreme point distribution of the signal. To solve this problem,~~ Wu and Huang (2009) proposed
85 the Ensemble Empirical Mode Decomposition (EEMD) method by adding different white noise in each
86 ensemble member to suppress mode mixing. Yeh et al. (2010) added two opposite-signal white noises to the
87 time-series data sequence, and proposed an improved algorithm for EEMD, Complete Ensemble Empirical
88 Mode Decomposition (CEEMD). The decomposition effect is equivalent to EEMD, and the reconstruction
89 error caused by adding white noise is reduced (Tang et al., 2015). At present, the EMD model and its

90 improved algorithms had been widely used in many fields on ocean science, such as storm surge and sea
91 level rise (Wu et al., 2011; Lee, 2013; Ezer and Atkinson, 2014), tidal amplitude (Cheng et al., 2017; Pan et
92 al., 2018) and wave height (Duan et al., 2016; Sadeghifar et al., 2017; López et al., 2017). These studies and
93 applications reflected that the EMD model and its improved algorithms can effectively reduce the non-
94 stationarity of the time-series data, which helps further analysis and processing.

95 The ensemble empirical mode decomposition (EEMD) method is a noise assisted empirical mode
96 decomposition algorithm. The CEEMD works by adding a certain amplitude of white noise to a time series,
97 decomposing it via EMD, and saving the result. In contrast to the EEMD method, the CEEMD also ensures
98 that the IMF set is quasi-complete and orthogonal. The CEEMD can ameliorate mode mixing and
99 intermittency problems. The CEEMD is a computationally expensive algorithm and may take significant
100 time to run.

101 For nonlinear prediction, the more commonly used methods are curve fitting (Motulsky and Ransnas,
102 1987), gray-box model (Pearson and Pottmann, 2000), homogenization function model (Monteiro et al.,
103 2008), neural network (Deo et al., 2001; Wang et al, 2015; Kim et al., 2016) and so on. Among them, Back-
104 Propagation Neural Network (BPNN) (Lee, 2004; Jain and Deo, 2006; Savitha and Al, 2017; Wang et al.,
105 2018) has certain advantages in dealing with nonlinear problems, it is a basic machine learning algorithm
106 and its principle is simple and operability is strong, so in ocean science and engineering it has been widely
107 used.

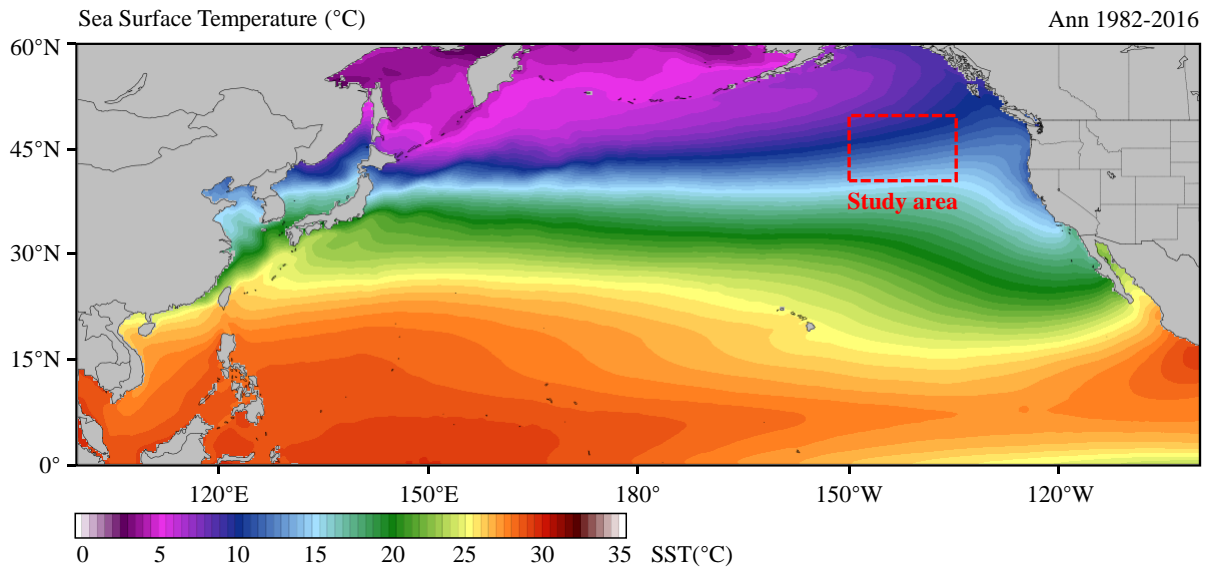
108 In view of non-stationary and nonlinear monthly mean SST, the EEMD, CEEMD and BP neural network
109 will be used here to study how to improve the accuracy of SST prediction. The hybrid EMD-BPNN models
110 will be established for the prediction of SSTA in the northeastern region of the Pacific Ocean.

111 **2 Data collection**

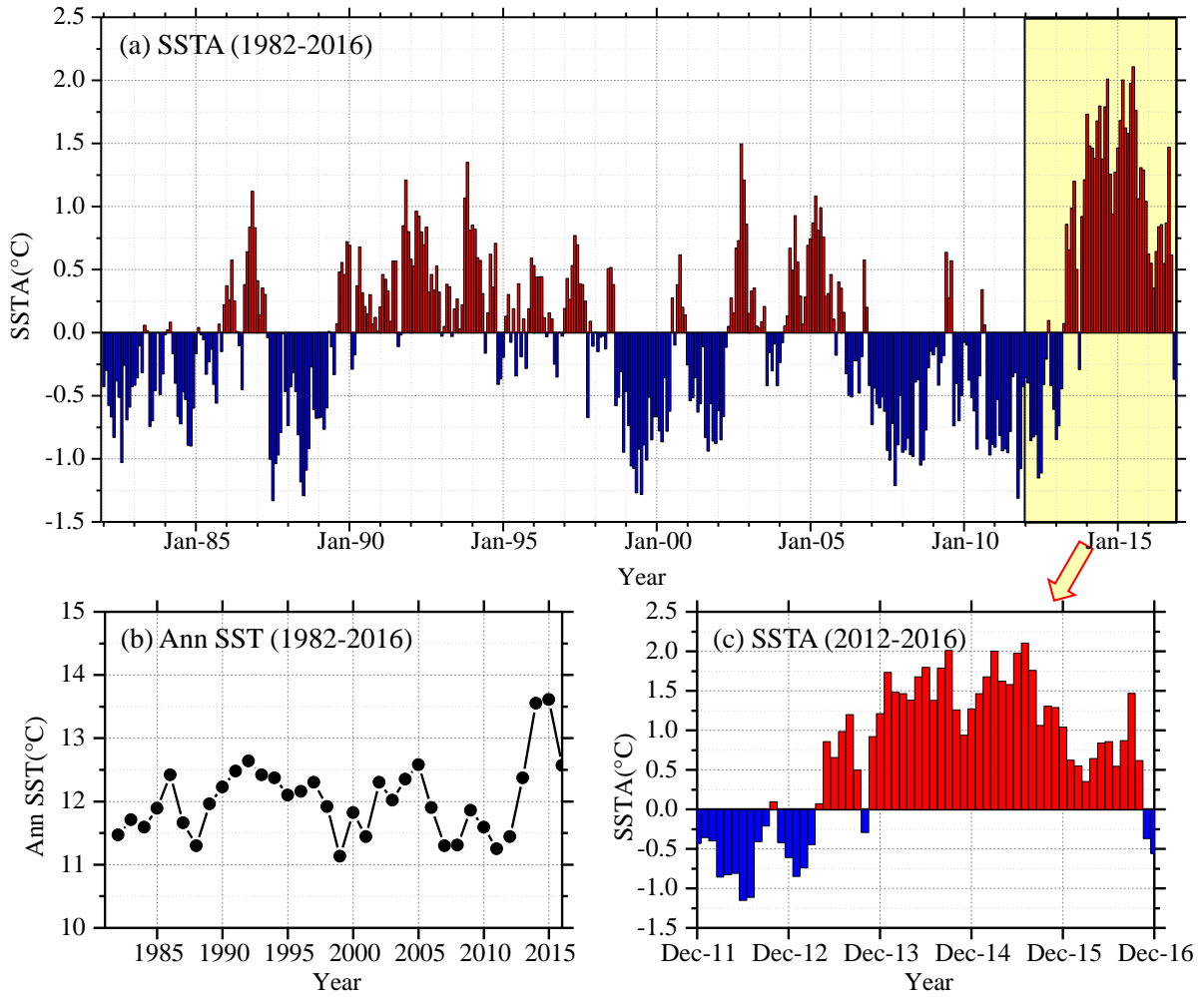
112 The SST time-series data in this study is from [the NOAA Optimum Interpolation Sea Surface](https://www.ncdc.noaa.gov/oisst/data-access)
113 [Temperature \(OISST\) official website \(Reynolds et al., 2007; Banzon et al., 2016;](https://www.ncdc.noaa.gov/oisst/data-access)
114 [https://www.ncdc.noaa.gov/oisst/data-access\)](https://www.ncdc.noaa.gov/oisst/data-access). The NOAA 1/4°daily OISST is an analysis constructed by
115 combining observations from different platforms (satellites, ships, buoys) on a regular global grid. There are
116 two kinds of OISST, named after the relevant satellite SST sensors. These are the Advanced Very High
117 Resolution Radiometer (AVHRR) and Advanced Microwave Scanning Radiometer on the Earth Observing
118 System (AMSR-E); the AVHRR dataset is used in this study. The average annual sea surface temperature in
119 North Pacific (0°N-60°N, 100°E-100°W) from January 1982 to December 2016 is shown in Fig.1.

120 It has been shown that the sea surface temperature anomaly in the northeastern Pacific in the ten years
121 2006-2016 was 2.0°C warmer than in the previous ten years 1996-2006. Previous studies (Bond et al., 2015)
122 showed that in the spring and summer of 2014, the high SST area of the northeastern Pacific had expanded
123 to coastal ocean waters, which affected the weather in coastal areas and the lives of fishermen, and even
124 affected the temperature in Washington, USA, causing interference to daily life.

125 In this study, we select the northeastern region of the North Pacific Ocean (in Fig.1, 40°N-50°N, 150°W-
126 135°W) to measure sea surface temperature. The time-series data of SST for the study area from January
127 1982 to December 2016 with a data length of 420 months was obtained from OISST-V2 (Fig. 2). The monthly
128 mean sea surface temperature anomaly (SSTA) was used in the analysis and calculation. As shown in Fig.
129 2(a), it can be found the overall time-series data is very messy, nonlinear and random from the perspective
130 of the image.



131
132 **Fig.1** Average annual sea surface temperature in North Pacific during Jan 1982 to Dec 2016 (35-years).



133

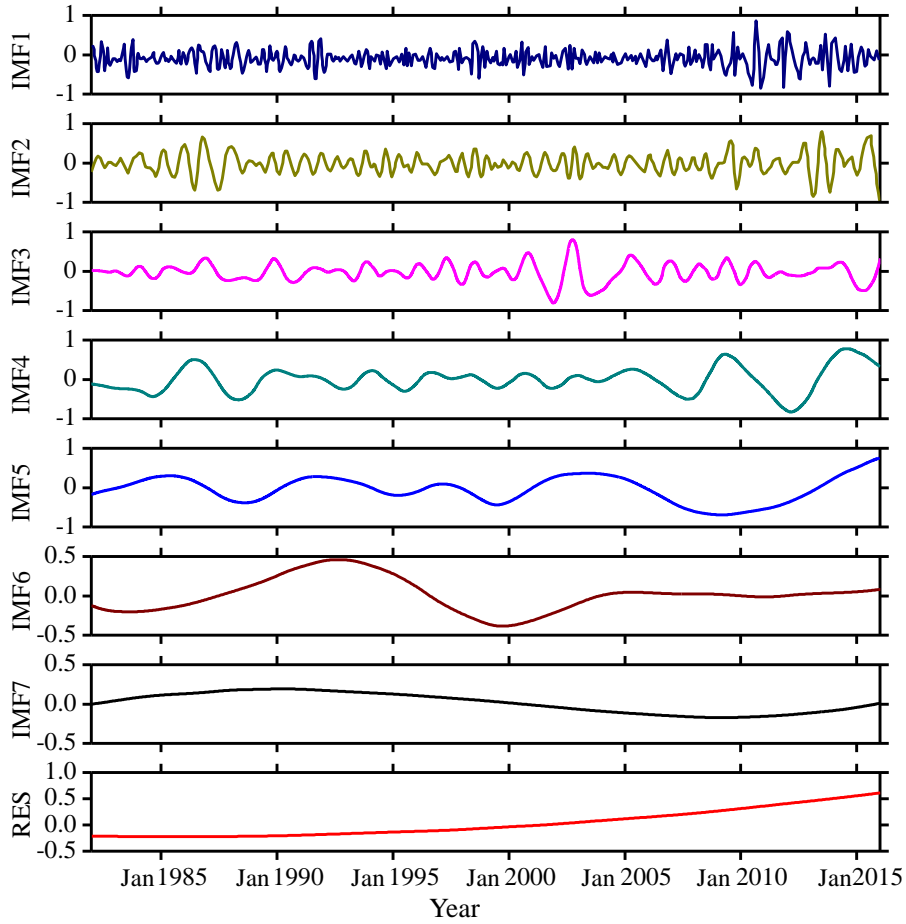
134 **Fig.2** The time-series of sea surface temperature in the study area. (a) SST anomaly (1982-2016, 35 years);
 135 (b) Annual SST (1982-2016, 35 years); (c) SST anomaly (2012-2016, 5 years).

136 **3 Decomposition of SSTA**

137 The purpose of this study is to combine the EEMD algorithm and the CEEMD decomposition algorithm
 138 respectively with the BP neural network algorithm to establish a prediction model, a hybrid EMD-BPNN
 139 model. The EEMD and CEEMD algorithms are performed on the monthly mean SSTA data to obtain a series
 140 of intrinsic mode functions (IMFi). Each IMFi is predicted by a BP neural network and then ~~each the~~ IMFi
 141 ~~are recombined~~ ~~is reconstructed~~ to obtain the predicted value of SSTA.

142 **3.1 Decomposition by the EEMD algorithm**

143 The SSTA in Fig. 2(a) has been decomposed based on the ensemble empirical mode decomposition
 144 (EEMD algorithm), and seven IMF components and a residual component RES (Residue) are obtained as
 145 shown in Fig. 3.



146

147 **Fig.3** IMF components and the trend item RES of monthly mean SSTA over the study area based on the
 148 EEMD algorithm during 1982-2016.

149

150 It can be seen from Fig. 3 that the first three intrinsic mode function components IMF1, IMF2, and IMF3

151 still exhibit strong ~~nonlinearity and~~ non-stationarity because they have strong irregular oscillations and

152 periodic changes. The IMF4 to IMF7 and the final trend term RES have some periodicity and relatively

153 regular fluctuation, and the non-stationary ~~and nonlinear~~ properties are less than the first three components.

154 The trend term RES reflects that the overall trend of SSTA has gradually increased since 1982. As the non-

155 stationarity of ~~each~~ IMF_i decreases with increasing i is gradually reduced, the EEMD algorithm will reduce

156 the influence of non-stationarity on prediction. The absolute error (ERR) of the decomposition can be ~~en~~

157 calculated by the following Formula (1).

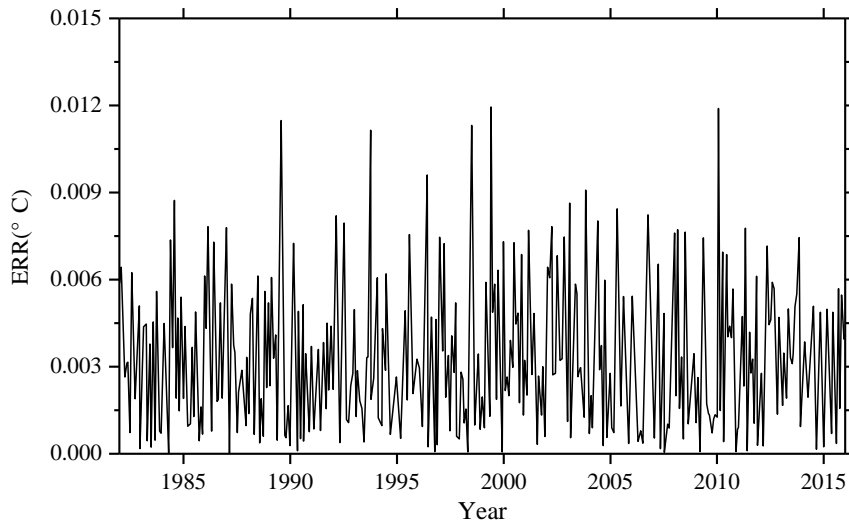
$$158 \quad a(t) = \left| S(t) - \left[\sum_{i=1}^7 I_i(t) + R(t) \right] \right| \quad (1)$$

159 where, $a(t)$ is the absolute error (ERR), $S(t)$ the original SSTA observation data, $I_i(t)$ the i -th component

160 of the IMF (IMF_i), and $R(t)$ the trend term (RES).

161 The absolute error (ERR) based on the EEMD algorithm is shown in Fig. 4. It can be seen from the
162 figure that the ERR of 420 months after decomposition is basically below 0.01 °C, and the ERR exceeds
163 0.01 °C in five months: June 1989, September 1993, July 1998, May 1999 and March 2010.

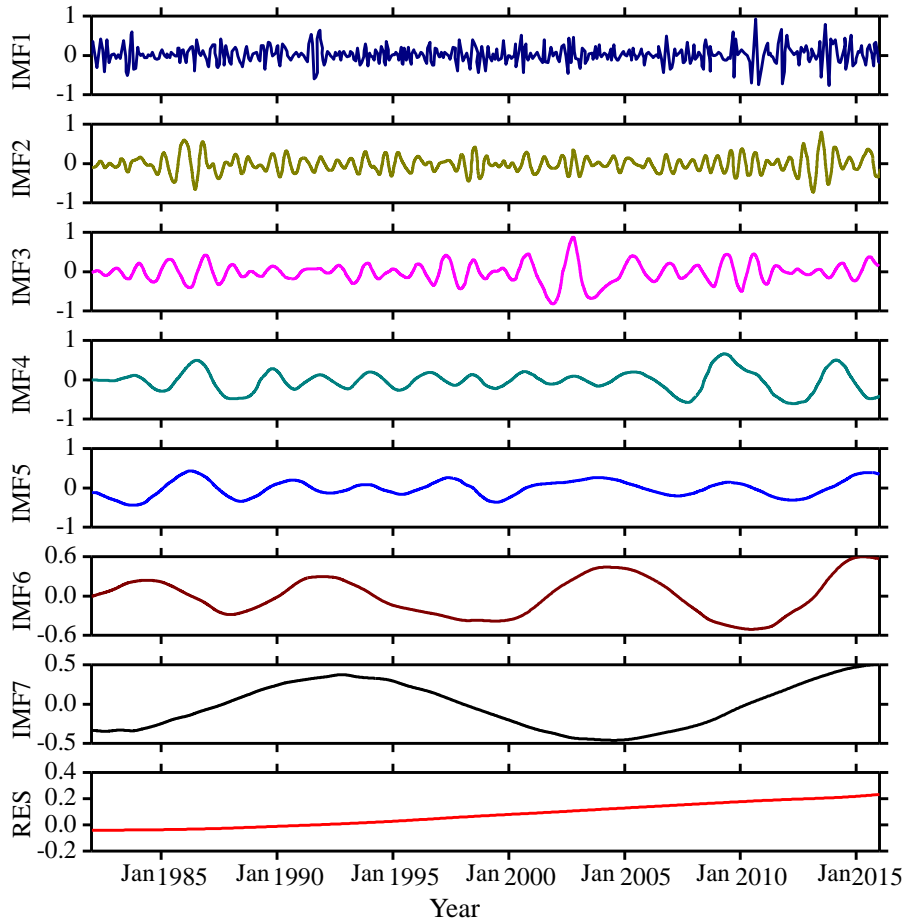
164 In addition to June 1989, the other four monthly data with a large ERR occurred during the El Niño
165 period. The maximum error is in March 2010, the actual value is -0.1204 °C, the result based on EEMD
166 algorithm is -0.1325 °C, the ERR of decomposition is 0.0121 °C; the minimum error, in April 1987, is
167 1.73×10^{-5} °C. The overall mean ERR based on the EEMD algorithm is 0.0035 °C ~~and the order of magnitude~~
168 ~~is 10^{-3} .~~



169
170 **Fig. 4** The ERR of monthly mean SSTA over the study area based on the EEMD algorithm during 1982-2016.

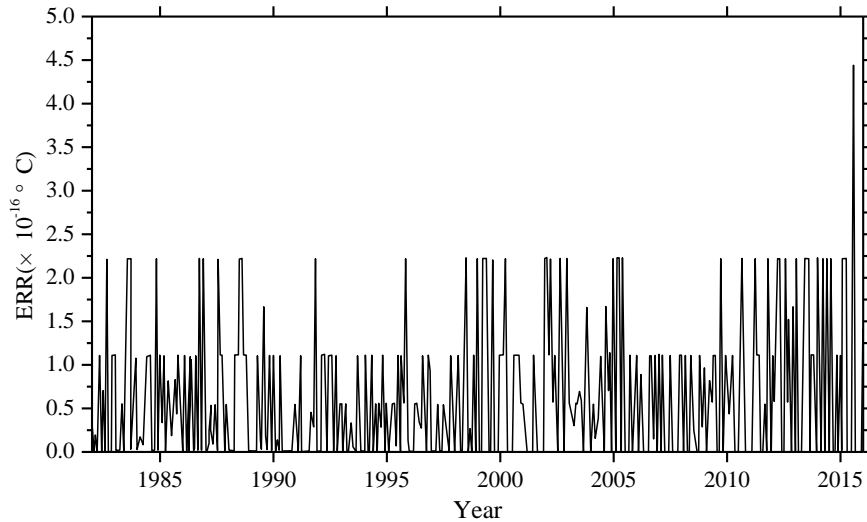
171
172 **3.2 Decomposition by the CEEMD algorithm**

173 The SSTA has been decomposed based on the complementary ensemble empirical mode decomposition
174 (CEEMD algorithm) and seven IMF components and a residual component RES (Residue) are obtained as
175 shown in Fig. 5. It can be seen when comparing the decomposition results based on EEMD and CEEMD
176 algorithms that although the mode components decomposed by CEEMD algorithm are different from the
177 corresponding results decomposed by EEMD, the ~~non-linearities and~~ non-stationarities of the eightseven
178 modes decomposed by the two decomposition algorithms are gradually decreasing, and the final trend term
179 RES is an upward trend. Both decomposition algorithms confirm the characteristic of a gradual increase in
180 the overall trend of the data series.



181
 182 **Fig.5** IMF components and the trend item RES of monthly mean SSTA over the study area based on the
 183 CEEMD algorithm during 1982-2016.

184
 185 The absolute error (ERR) obtained based on the CEEMD algorithm is shown in Fig. 6. It can be seen
 186 from the figure that the ERR of 420 months data after decomposition is less than $5 \times 10^{-16} \text{ } ^\circ\text{C}$, and the accuracy
 187 is very better. The maximum error is $4.48 \times 10^{-16} \text{ } ^\circ\text{C}$ in March 2016; the minimum error is zero. The overall
 188 mean ERR based on CEEMD algorithm is $6.10 \times 10^{-17} \text{ } ^\circ\text{C}$ ~~and the order of magnitude is 10^{-17}~~ . By comparing
 189 the results and errors of the above two decomposition algorithms, it can be seen that the error based on the
 190 improved algorithm (CEEMD) is much smaller than the error based on the EEMD algorithm. Because more
 191 white noise with the opposite sign had been added in CEEMD algorithm, the reconstruction error caused
 192 by the white noise has been reduced over it in EEMD algorithm.



193

194 **Fig. 6** The ERR of monthly mean SSTA over the study area based on the CEEMD algorithm during 1982-
 195 2016.

196

197 **4 SSTA prediction model**

198 **4.1 The BP neural network**

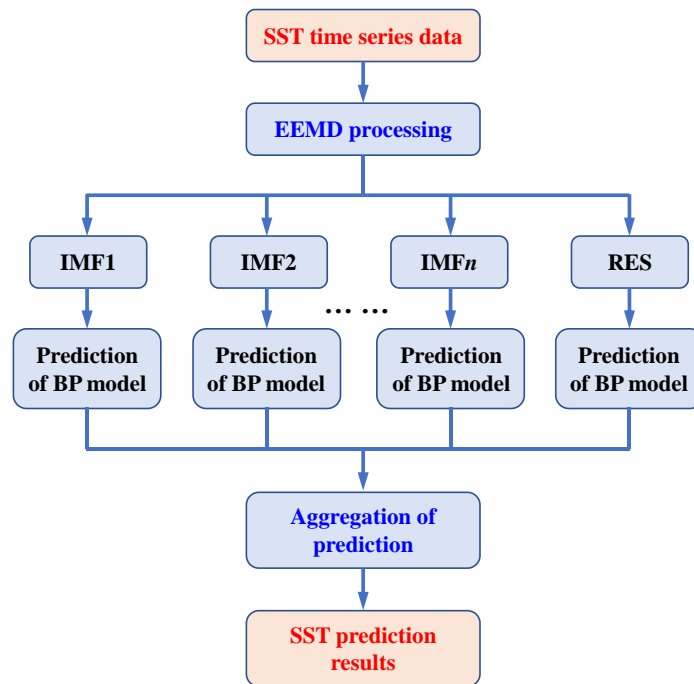
199 Artificial Neural Network (ANN) is an information processing approach based on the biological neural
 200 network (López et al., 2015; Kim et al., 2016). In theory, ANN can simulate any complex nonlinear
 201 relationship through nonlinear units (neurons) and has been widely used in the prediction area, such as wave
 202 height and storm surge. The most basic structure of ANN consists of input layers, hidden layers and output
 203 layers. One of the most widely used ANN models is the back propagation neural network (BPNN, Wang et
 204 al., 2018) algorithm based on the BP algorithm.

205 The BPNN algorithm is a multi-layer feedforward network trained according to the error back
 206 propagation algorithm and is one of the most widely used deep learning algorithms. The BP network can be
 207 used to learn and store a large number of mappings of input and output models without the need to publicly
 208 describe the mathematical equations of these mapping relationships. The learning rule is to use the steepest
 209 descent method. When applied to SST predicting, the input data are monthly mean SST in previous months
 210 and the output data are predicted SST time-series data. The desired data for comparison is the observed actual
 211 SST.

212 **4.2 SSTA prediction model based on hybrid improved EMD-BPNN algorithm**

213 The proposed monthly mean sea surface temperature anomaly (SSTA) predicting model includes three

214 steps as follows. First, original SST datasets are decomposed into certain more stationary signals with
 215 different frequencies by EEMD. Second, the BP neural network is used to predict each IMF and the residue
 216 RES. A rolling forecasting process is studied. The prediction is made using the previous data for one step
 217 ahead. Finally, the prediction results of each IMF and the residue RES are aggregated to obtain the final SST
 218 prediction results. The flowchart of the SST prediction model based on hybrid improved empirical mode
 219 decomposition algorithm (improved EMD algorithm) and back-propagation neural network (BPNN) is shown
 220 in Fig. 7. The SST prediction model has been abbreviated as a hybrid improved EMD-BPNN model in the
 221 following article.



222
 223 **Fig.7** The flowchart of SST prediction model based on hybrid improved empirical mode decomposition
 224 algorithm (improved EMD algorithm) and back-propagation neural network (BPNN).

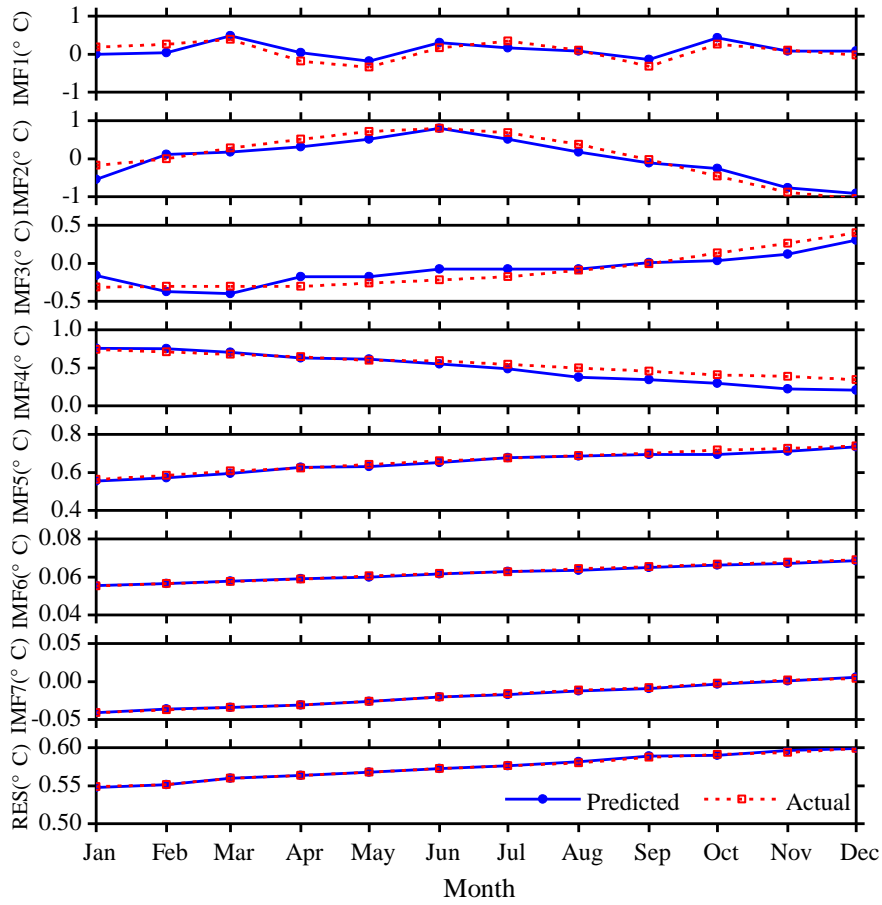
225
 226 **5 Case study: SSTA prediction based on the hybrid improved EMD-BPNN models**

227 In order to study the effects of the two improved EMD algorithms (EEMD and CEEMD) on the
 228 prediction results, and to analyze the prediction ability of BP neural network, the following experiments were
 229 carried out. Predict SSTA results in 2017 and analyze the prediction abilities of different mode decomposition
 230 data based on EEMD and CEEMD algorithms. The experiment content is as follows: the BP neural network
 231 is trained with the decomposition data of each mode from 1982 to 2016, and the SSTA in 2017 is predicted
 232 by the trained neural network, and the observation results of 12 months in 2017 are used to compare and

233 analyze with the prediction results.

234 ~~Since the nonlinearity of the IMF1 to IMF3 is still relatively strong, a~~ three-layer BP neural network
 235 structure has been chosen and independently analyze and predict each month. For the IMF4 and subsequent
 236 modes, ~~since the nonlinearity and the~~ non-stationarity have been degraded relative to the first three modes, a
 237 BP neural network with 12 nodes at input layer and output layer has been used to train and predict SSTA.

238 The prediction results of each mode decomposition component based on the EEMD algorithm are shown
 239 in Fig. 8. The absolute errors of the predicted value and the actual value are shown in Table 1.



240
 241 **Fig. 8** SSTA prediction results based on the hybrid EEMD-BPNN model of each individual component in
 242 2017.

243 Root mean square error (RMSE) is used as metrics to access the performance of the two different models.

$$244 \quad \text{RMSE} = \sqrt{\frac{1}{N} \sum_{n=1}^N (x_n - y_n)^2} \quad (2)$$

245 where, x_n and y_n are the observed and the predicted values respectively, N is the number of data used for
 246 the performance evaluation and N is 12 in this study. Results are shown in Table 1.

247

248 **Table 1.** The absolute errors ERRs of the SSTA prediction results of each individual component based on the
 249 hybrid EEMD-BPNN model (unit: °C).

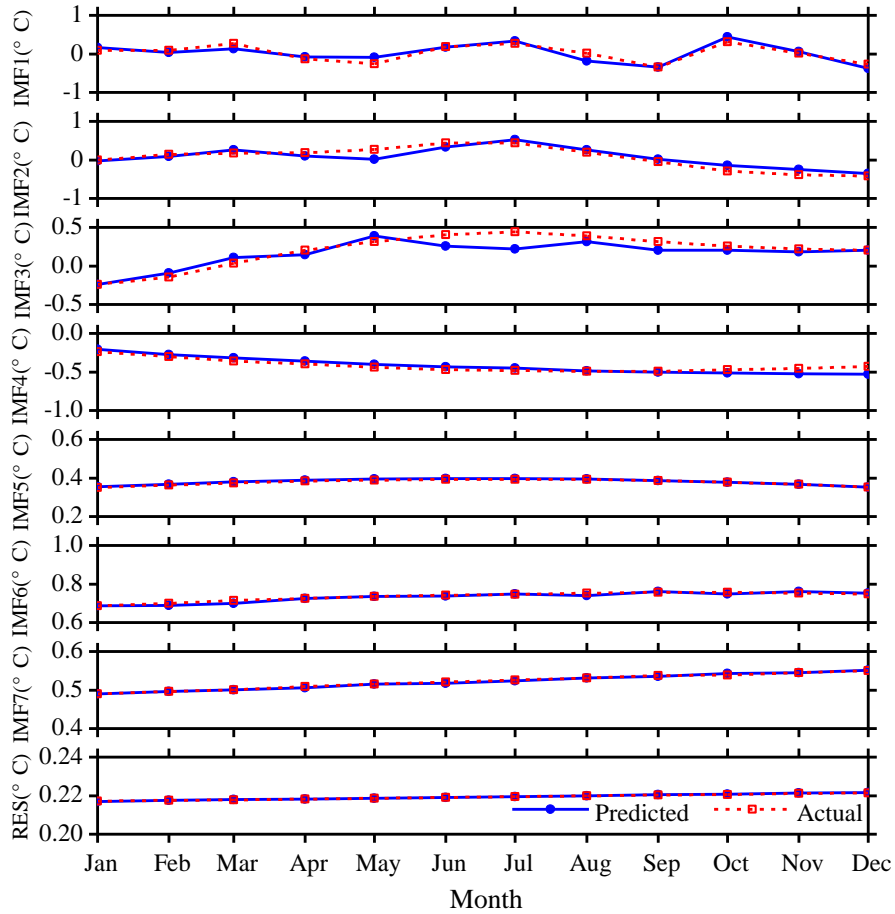
	Max ERR	Min ERR	Mean ERR	RMSE
IMF1	0.2197	0.0014	0.1424	0.1486
IMF2	0.2166	0.0323	0.1297	0.1673
IMF3	0.1872	0.0051	0.1070	0.1245
IMF4	0.1602	1.6869×10^{-4}	0.0663	0.0857
IMF5	0.0158	0.0010	0.0089	0.0104
IMF6	3.8766×10^{-4}	1.9752×10^{-4}	2.7221×10^{-4}	0.0003
IMF7	5.2662×10^{-4}	1.6387×10^{-4}	1.7907×10^{-4}	0.0002
RES	5.4859×10^{-4}	2.2308×10^{-4}	2.4766×10^{-4} <u>2.7766×10^{-4}</u>	0.0002 <u>0.0003</u>

250
 251 It can be seen from Fig. 8 and Table 1 that the maximum absolute error (Max ERR) of the first
 252 decomposition component IMF1 based on the hybrid EEMD-BPNN model is 0.2197 °C in January. The
 253 minimum absolute error (Min ERR) is 0.0014 °C, which is in August. The prediction ability of the second
 254 mode decomposition component IMF2 is roughly equivalent to the IMF1, and the mean absolute error (Mean
 255 ERR) of the first three intrinsic mode function components IMF1, IMF2, and IMF3 are between 0.10 °C and
 256 0.15 °C. The mean absolute errors of the IMF4 and IMF5 are 0.0663 °C and 0.0089 °C, respectively, and the
 257 prediction accuracy based on the hybrid EEMD-BPNN model is roughly equivalent to the decomposition
 258 accuracy of the EEMD algorithm. The prediction errors of the last two intrinsic mode function components
 259 and the residue RES are on the order of 10^{-4} . It can be seen that as the ~~nonlinearity and~~ non-stationarity of
 260 the series data decreases, the error of the prediction results becomes smaller and smaller.

261 According to the same method, the eight mode components decomposed by CEEMD algorithm have
 262 been analyzed and predicted. The prediction results and error analysis have been shown in Fig. 9 and Table
 263 2. It can be seen from Fig. 9 and Table 2 that the maximum error of the first decomposition component IMF1
 264 based on the hybrid CEEMD-BPNN model is 0.1779 °C in May. The minimum error is 0.0068 °C, which is
 265 in June.

266 The prediction ability of the second mode decomposition component IMF2 is roughly equivalent to the
 267 IMF1. Except for the four months of May, September, October, and November, the accuracies of prediction
 268 results of other months are satisfactory. The prediction results of the first three intrinsic mode function

269 components IMF1, IMF2, and IMF3 are basically the same as the actual data. In the prediction results of the
 270 fourth mode component IMF4, except for a slight error in December, the prediction ability is better. The
 271 predicted results of the last three intrinsic mode function components IMF5, IMF6, IMF7 and the residue
 272 RES are basically consistent with the observation results.

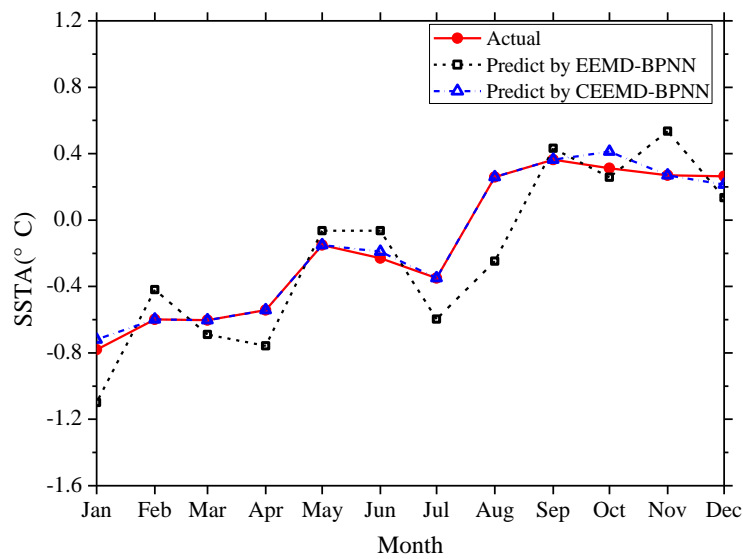


273
 274 **Fig. 9** SSTA prediction results based on the hybrid CEEMD-BPNN model of each individual component in
 275 2017.
 276

277 **Table 2.** The absolute errors ERRs of the SSTA prediction results of each individual component based on the
 278 hybrid CEEMD-BPNN model (unit: °C).

	Max ERR	Min ERR	Mean ERR	RMSE
IMF1	0.1779	0.0068	0.0827	0.0987
IMF2	0.1643	0.0413	0.0811	0.1124
IMF3	0.1521	0.0160	0.0713	0.1006
IMF4	0.0851	0.0211	0.0324	0.0427
IMF5	0.0052	8.7694×10^{-5}	0.0021	0.0029
IMF6	0.0103	5.7748×10^{-5}	0.0043	0.0056
IMF7	0.0017	3.6026×10^{-5}	9.1374×10^{-4}	0.0010
RES	3.0342×10^{-5}	2.0163×10^{-6}	1.1572×10^{-5}	1.5017×10^{-5}

279
 280 The prediction results of the monthly mean SSTA in 2017 are obtained by reconstructing the mode
 281 decomposition components (Fig. 10) and the absolute error (ERR) of prediction results have been shown in
 282 Table 3. It can be seen from the figure and table that the prediction results based on the EEMD-BPNN model
 283 have larger ERRs in January and August, exceeding 0.3 °C, and the accuracies of prediction results in other
 284 months are satisfactory (the ERR is less than 0.3). The prediction accuracy based on the CEEMD-BPNN
 285 model is satisfactory, except for the ERR exceeding 0.1 °C in October, and the prediction ability based on
 286 the CEEMD-BPNN model is generally better than that of the EEMD-BPNN model.



287
 288 **Fig. 10** Monthly SSTA prediction results based on the hybrid improved EMD-BPNN models in 2017.

289 **Table 3.** The absolute errors ERRs of the SSTA prediction results based on the two different hybrid improved
 290 EMD-BPNN models (unit: °C).

	EEMD-BPNN model	CEEMD-BPNN model		EEMD-BPNN model	CEEMD-BPNN model
Jan	0.3188	0.0623	Sep	0.0687	0.0132
Feb	0.1780	0.0103	Oct	0.0545	0.1607
Mar	0.0867	0.0063	Nov	0.2651	0.0101
Apr	0.2153	0.0137	Dec	0.1290	0.0183
May	0.0854	0.0102	Min ERR	0.0545	0.0063
Jun	0.1662	0.0224	Max ERR	0.5068	0.1607
Jul	0.2474	0.0077	Mean ERR	0.1935	0.0289
Aug	0.5068	0.0112	RMSE	0.2299	0.0512

291
 292 The correlation coefficient between the prediction values based on the CEEMD-BPNN model and
 293 observations is 0.97 indicating a significance level of 0.001. ~~shown that the value of the correlation~~
 294 ~~coefficient that indicates a significance level of 0.001 and the correlation coefficient reached 0.97.~~ The result
 295 indicates that SSTA in 2017 ~~had been~~ was predicted accurately by the CEEMD-BPNN model. As can be seen
 296 from the above discussions, the ERR of decomposition components based on the EEMD and CEEMD
 297 algorithms will affect the accuracy of the final prediction results. Table 3 shows that ~~predicting prediction~~
 298 results of the hybrid CEEMD and BPNN model are much better than with the EEMD-BPNN. ~~ameliorated a~~
 299 ~~lot as compared to the EEMD-BPNN direct predicting model.~~ This is because after CEEMD, the original
 300 unsteady ~~and nonlinear~~ data are changed into certain components that have fixed frequency and periodicity.
 301 The CEEMD algorithm with less decomposition error has less error in the final prediction results, which
 302 proves that the CEEMD method has more advantages in data decomposition than the EEMD method. At the
 303 same time, we can find that the final prediction error of the two prediction models mainly comes from the
 304 first three mode decomposition components, and the error of the last five components has little effect on the
 305 accuracy of the final prediction results.

306
 307 **6 Conclusions**

308 This paper presents an SST predicting method based on the hybrid EMD algorithms and BP neural
 309 network method to process the SST data with nonlinearity and non-stationarity. Through EEMD and CEEMD

310 algorithms, SSTA time-series data are decomposed into different IMFs and a residue RES. BP neural network
311 is applied to predict individual IMFs and the residue RES. Final results can be obtained by adding the
312 predicting results of individual IMFs and RES.

313 In order to illustrate the effectiveness of the proposed approach, a case study was carried out. SSTA
314 prediction results based on the hybrid EEMD-BPNN model and the hybrid CEEMD-BPNN model are
315 discussed ~~respectively~~. In comparison, the proposed hybrid CEEMD-BPNN model is much better and its
316 prediction results are more accurate.

317 From the absolute error of the prediction results of each component IMF and the absolute error of the
318 predicted SSTA, the prediction error of SSTA mainly comes from the prediction of the first three mode
319 decomposition components (IMF1, IMF2 and IMF3), ~~because the first three mode components still have~~
320 ~~strong nonlinearity and non-stationarity. As the nonlinearity gradually decreases, the absolute error of the~~
321 ~~prediction results gradually decreases.~~

322 SST prediction has been only preliminary ~~carried out~~, based on the two improved EMD algorithms and
323 BP neural network in this paper. The results show that the hybrid CEEMD-BPNN model is more accurate in
324 predicting SST. This work can provide a reference for predicting SST and El Niño in the future. In the follow-
325 up study, how to improve the forecast duration is the focus of this work.

326 It should be noted that some factors affecting the SST prediction results include: the length and interval
327 of the time series of the database, as well as different data sources because their values are also different. The
328 SST time-series data in this study is based on NOAA Optimum Interpolation Sea Surface Temperature
329 (OISST) datasets from January 1982 to December 2016.

330

331 **Acknowledgement**

332 This work was supported by National Natural Science Foundation of China (Grant Nos. 51809023,
333 51879015, 51839002, 51809021 and 51509023).

334

335 **References:**

336 Amezcua-Sanchez, J. P. and Adeli, H.: A new music-empirical wavelet transform methodology for time-
337 frequency analysis of noisy nonlinear and non-stationary signals, Digit. Signal Process., 45, 55-68,
338 <https://doi.org/10.1016/j.dsp.2015.06.013>, 2015.

339 Banzon, V., Smith, T. M., Chin, T. M., Liu, C., and Hankins, W.: A long-term record of blended satellite and

340 in situ sea-surface temperature for climate monitoring, modeling and environmental studies, *Earth Syst.*
341 *Sci. Data*, 8, 165-176, <https://doi.org/10.5194/essd-8-165-2016>, 2016.

342 Bond, N. A., Cronin, M. F., Freeland, H., and Mantua N.: Causes and impacts of the 2014 warm anomaly in
343 the NE Pacific. *Geophys. Res. Lett.*, 42, 3414-3420, <https://doi.org/10.1002/2015GL063306>, 2015.

344 Buckley, M. W., Ponte, R. M., Forget, G., and Heimbach, P.: Low-frequency SST and upper-ocean heat
345 content variability in the North Atlantic, *J. Climate*, 27, 4996-5018, [https://doi.org/10.1175/JCLI-D-13-](https://doi.org/10.1175/JCLI-D-13-00316.1)
346 00316.1, 2014.

347 Chen, C., Cane, M. A., Henderson, N., Lee, D. E., Chapman, D., Kondrashov D., and Chekroun, M. D.:
348 Diversity, nonlinearity, seasonality, and memory effect in ENSO simulation and prediction using
349 empirical model reduction, *J. Climate*, 29: 1809-1830, <https://doi.org/10.1175/JCLI-D-15-0372.1>,
350 2016b.

351 Chen, Z., Wen, Z., Wu, R., Lin X., and Wang J.: Relative importance of tropical SST anomalies in maintaining
352 the Western North Pacific anomalous anticyclone during El Niño to La Niña transition years, *Clim.*
353 *Dynam.*, 46, 1027-1041, <https://doi.org/10.1007/s00382-015-2630-1>, 2016a.

354 Cheng, Y., Ezer, T., Atkinson, L. P., and Xu, Q.: Analysis of tidal amplitude changes using the EMD method,
355 *Cont. Shelf Res.*, 148: 44-52, <https://doi.org/10.1016/j.csr.2017.09.009>, 2017.

356 Deo, M. C., Jha, A., Chaphekar, A. S., and Ravikant, K.: Neural networks for wave forecasting, *Ocean Eng.*,
357 28: 889-898, [https://doi.org/10.1016/S0029-8018\(00\)00027-5](https://doi.org/10.1016/S0029-8018(00)00027-5), 2001.

358 Duan, W. Y., Han, Y., Huang, L. M., Zhao, B. B., and Wang, M. H.: A hybrid EMD-SVR model for the short-
359 term prediction of significant wave height, *Ocean Eng.*, 124, 54-73,
360 <https://doi.org/10.1016/j.oceaneng.2016.05.049>, 2016.

361 Duan, W., Huang, L., Han Y., and Huang D.: A hybrid EMD-AR model for nonlinear and non-stationary
362 wave forecasting, *J Zhejiang Univ-Sc A*, 17(2): 115-129, <https://doi.org/10.1631/jzus.A1500164>, 2016.

363 Ezer, T. and Atkinson, L. P.: Accelerated flooding along the US East Coast: on the impact of sea - level rise,
364 tides, storms, the Gulf Stream, and the North Atlantic oscillations, *Earths Future*, 2, 362-382,
365 <https://doi.org/10.1002/2014EF000252>, 2014.

366 Griffies, S. M., Winton, M., Anderson, W. G., Benson, R., Delworth, T. L., Dufour, C. O., Dunne, J. P.,
367 Goddard, P., Morrison, A. K., Rosati, A., Wittenberg, A. T., Yin, J., and Zhang, R.: Impacts on ocean
368 heat from transient mesoscale eddies in a hierarchy of climate models. *J. Climate*, 28, 952-977,
369 <https://doi.org/10.1175/JCLI-D-14-00353.1>, 2015.

370 He, J., Deser, C., and Soden, B. J.: Atmospheric and oceanic origins of tropical precipitation variability. *J.*
371 *Climate*, 30, 3197-3217, <https://doi.org/10.1175/JCLI-D-16-0714.1>, 2017.

372 Huang, N. E., Shen, Z., Long, S. R., Wu, M. C., Shih, H. H., Zheng, Q., Yen, N., Tung, C. C., and Liu, H. H.:
373 The empirical mode decomposition and the Hilbert spectrum for nonlinear and non-stationary time
374 series analysis, *P. Roy. Soc. A-Math. Phys.*, 454, 903-995. <https://doi.org/10.1098/rspa.1998.0193>, 1998.

375 Huang, N. E. and Wu, Z.: A review on Hilbert - Huang transform: Method and its applications to geophysical
376 studies, *Rev. Geophys.*, 46, RG2006, <https://doi.org/10.1029/2007RG000228>, 2008.

377 Hudson, D., Alves, O., Hendon, H. H., Wang, G.: The impact of atmospheric initialisation on seasonal
378 prediction of tropical Pacific SST, *Clim. Dynam.*, 36, 1155-1171, [https://doi.org/10.1007/s00382-010-](https://doi.org/10.1007/s00382-010-0763-9)
379 [0763-9](https://doi.org/10.1007/s00382-010-0763-9), 2011.

380 Jain, P. and Deo, M. C.: Neural networks in ocean engineering, *Ships Offshore Struc.*, 1, 25-35,
381 <https://doi.org/10.1533/saos.2004.0005>, 2006.

382 Khan, M. Z. K., Sharma, A., and Mehrotra, R.: Global seasonal precipitation forecasts using improved sea
383 surface temperature predictions, *J Geophys. Res. -Atmos.*, 122, 4773-4785,
384 <https://doi.org/10.1002/2016JD025953>, 2017,

385 Kim, Y., Kim, H., and Ahn, I. G.: A study on the fatigue damage model for Gaussian wideband process of
386 two peaks by an artificial neural network, *Ocean Eng.*, 111, 310-322,
387 <https://doi.org/10.1016/j.oceaneng.2015.11.008>, 2016.

388 Kumar, M., Parmar, C., Chaudhary, V., Kumar, A., and SST-1 team.: Observation of plasma shift in SST-1
389 using optical imaging diagnostics, *J Phys. Conf. Ser.*, 823, 012056, [https://doi.org/10.1088/1742-](https://doi.org/10.1088/1742-6596/823/1/012056)
390 [6596/823/1/012056](https://doi.org/10.1088/1742-6596/823/1/012056), 2017.

391 Lee, H. S.: Estimation of extreme sea levels along the Bangladesh coast due to storm surge and sea level rise
392 using EEMD and EVA, *J Geophys. Res.-Oceans*, 118, 4273-4285, <https://doi.org/10.1002/jgrc.20310>,
393 2013,

394 Lee, T. L.: Back-propagation neural network for long-term tidal predictions, *Ocean Eng.*, 31, 225-238,
395 [https://doi.org/10.1016/S0029-8018\(03\)00115-X](https://doi.org/10.1016/S0029-8018(03)00115-X), 2004.

396 López, I., Aragonés, L., Villacampa, Y., and Serra, J. C.: Neural network for determining the characteristic
397 points of the bars, *Ocean Eng.*, 136: 141-151, <https://doi.org/10.1016/j.oceaneng.2017.03.033>, 2017.

398 Monteiro, E., Yvonnet, J., He, Q. C.: Computational homogenization for nonlinear conduction in
399 heterogeneous materials using model reduction. *Comp. Mater. Sci.*, 42, 704-712,

400 <https://doi.org/10.1016/j.commatsci.2007.11.001>, 2008.

401 Motulsky, H. J. and Ransnas, L. A.: Fitting curves to data using nonlinear regression: a practical and
402 nonmathematical review, *Faseb J.*, 1, 365-374. <https://doi.org/10.1096/fasebj.1.5.3315805>, 1987.

403 Pan, H., Guo, Z., Wang, Y., and Lv, X.: Application of the EMD method to river tides, *J. Atmos. Ocean. Tech.*,
404 35, 809-819, <https://doi.org/10.1175/JTECH-D-17-0185.1>, 2018.

405 Pearson, R. K. and Pottmann, M.: Gray-box identification of block-oriented nonlinear models, *J. Process*
406 *Contr.*, 10, 301-315, [https://doi.org/10.1016/S0959-1524\(99\)00055-4](https://doi.org/10.1016/S0959-1524(99)00055-4), 2000.

407 Reynolds, R. W., Smith, T. M., Liu, C., Chelton, D. B., Casey, K. S., and Schlax, M. G.: Daily high-
408 resolution-blended analyses for sea surface temperature, *J. Climate*, 20, 5473-5496,
409 <https://doi.org/10.1175/2007JCLI1824.1>, 2007.

410 Sadeghifar, T., Motlagh, M. N., Azad, M. T., and Mahdizadeh, M. M.: Coastal wave height prediction using
411 Recurrent Neural Networks (RNNs) in the south Caspian Sea, *Mar. Geod.*, 40, 454-465,
412 <https://doi.org/10.1080/01490419.2017.1359220>, 2017.

413 Savitha, R. and Mamun, A. A.: Regional ocean wave height prediction using sequential learning neural
414 networks, *Ocean Eng.*, 129: 605-612, <https://doi.org/10.1016/j.oceaneng.2016.10.033>, 2017.

415 Sukresno, B., Hanintyo, R., Kusuma, D. W., Jatisworo, D., and Murdimanto, A.: Three-way error analysis
416 of sea surface temperature (SST) between HIMAWARI-8, buoy, and mur SST in SAVU Sea, *Int. J.*
417 *Remote Sens. Earth Sci.*, 15, 25-36, <https://doi.org/10.30536/j.ijreses.2018.v15.a2855>, 2018,

418 Takakura, T., Kawamura, R., Kawano, T., Ichiyangi, K., Tanoue, M., and Yoshimura, K.: An estimation of
419 water origins in the vicinity of a tropical cyclone's center and associated dynamic processes, *Clim.*
420 *Dynam.*, 50, 555-569, <https://doi.org/10.1007/s00382-017-3626-9>, 2018.

421 Tang, L., Dai, W., Yu, L., and Wang, S.: A novel CEEMD-based EELM ensemble learning paradigm for crude
422 oil price forecasting, *Int. J. Inf. Tech. Decis.*, 14, 141-169, <https://doi.org/10.1142/S0219622015400015>,
423 2015.

424 Wang, S., Zhang, N., Wu, L., and Wang, Y.: Wind speed forecasting based on the hybrid ensemble empirical
425 mode decomposition and GA-BP neural network method, *Renew. Energ.*, 94, 629-636,
426 <https://doi.org/10.1016/j.renene.2016.03.103>, 2016.

427 Wang, W., Chau, K., Xu, D., and Chen, X.: Improving forecasting accuracy of annual runoff time series using
428 ARIMA based on EEMD decomposition, *Water Resour. Manag.*, 29, 2655-2675,
429 <https://doi.org/10.1007/s11269-015-0962-6>, 2015.

430 Wang, W., Tang, R., Li, C., Liu, P., and Luo, L.: A BP neural network model optimized by Mind Evolutionary
431 Algorithm for predicting the ocean wave heights, *Ocean Eng.*, 162, 98-107,
432 <https://doi.org/10.1016/j.oceaneng.2018.04.039>, 2018.

433 Wang, Y., Wilson, P. A., Zhang, M., and Liu, X.: Adaptive neural network-based backstepping fault tolerant
434 control for underwater vehicles with thruster fault, *Ocean Eng.*, 110, 15-24,
435 <https://doi.org/10.1016/j.oceaneng.2015.09.035>, 2015.

436 Wiedermann, M., Donges, J. F., Handorf, D., Kurths, J., and Donner, R. V.: Hierarchical structures in
437 Northern Hemispheric extratropical winter ocean–atmosphere interactions, *Int. J. Climatol.*, 37, 3821-
438 3836, <https://doi.org/10.1002/joc.4956>, 2017.

439 Wu, L. C., Kao, C. C., Hsu, T. W., Jao K. C. and Wang, Y. F.: Ensemble empirical mode decomposition on
440 storm surge separation from sea level data, *Coast. Eng. J.*, 53, 223-243,
441 <https://doi.org/10.1142/S0578563411002343>, 2011.

442 Wu Z., Schneider E. K. and Kirtman B. P.: The modulated annual cycle: an alternative reference frame for
443 climate anomalies, *Clim. Dyna.*, 31(7-8): 823-841, <https://doi.org/10.1007/s00382-008-0437-z>, 2008.

444 Wu, Z. and Huang, N. E.: Ensemble empirical mode decomposition: a noise-assisted data analysis method,
445 *Adv. Adap. Data Anal.*, 1, 1-41, <https://doi.org/10.1142/S1793536909000047>, 2009.

446 Wu Z., Jiang C., Chen J., Long Y., Deng B. and Liu X.: Three-Dimensional Temperature Field Change in the
447 South China Sea during Typhoon Kai-Tak (1213) Based on a Fully Coupled Atmosphere–Wave–Ocean
448 Model, *Water*, 11(1): 140, <https://doi.org/10.3390/w11010140>, 2019a.

449 Wu Z., Jiang C., Deng B., Chen J., Long Y., Qu K. and Liu X.: Numerical investigation of Typhoon Kai-tak
450 (1213) using a mesoscale coupled WRF-ROMS model, *Ocean Eng.*, 175: 1-15.
451 <https://doi.org/10.1016/j.oceaneng.2019.01.053>, 2019b.

452 Yeh, J. R., Shieh, J. S., and Huang, N. E.: Complementary ensemble empirical mode decomposition: A novel
453 noise enhanced data analysis method, *Adv. Adap. Data Anal.*, 2, 135-156,
454 <https://doi.org/10.1142/S1793536910000422>, 2010.

455 Zheng, X. T., Xie, S. P., Lv, L. H., and Zhou, Z. Q.: Intermodel uncertainty in ENSO amplitude change tied
456 to Pacific Ocean warming pattern, *J. Climate*, 29, 7265-7279, <https://doi.org/10.1175/JCLI-D-16-0039.1>,
457 2016.

458 Zhu, J., Huang, B., Kumar, A., and Kinter, J. L.: Seasonality in prediction skill and predictable pattern of
459 tropical Indian Ocean SST, *J. Climate*, 28, 7962-7984, <https://doi.org/10.1175/JCLI-D-15-0067.1>, 2015.